

# FDTD for Nanoscale and Optical Problems

© EYEWIRE

*Bartłomiej Salski, Malgorzata Celuch,  
and Wojciech Gwarek*

Scientific and engineering research are often looking in opposite directions. On the one hand, it seems scientifically elegant to cast all knowledge into a general theory of everything [1]. On the other hand, the huge progress that is taking place in both theory and technologies naturally imposes specialization and pushes knowledge into very specific and unique languages. Consequently, people from distinct research

areas often speak about similar phenomena using different terminologies. This makes their knowledge less portable and harder to disseminate beyond their own communities.

Electromagnetics (EMs) is a very good example of such tendencies. In principle, it spans a vast frequency range from dc up to at least the X-ray spectrum. In practice, except for very fundamental notions, it is hard to find a common technical language between,

---

*Bartłomiej Salski, Malgorzata Celuch (m.celuch@ire.pw.edu.pl), and Wojciech Gwarek are with the Institute of Radioelectronics, Warsaw University of Technology, ul. Nowowiejska 15/19, 00-665 Warsaw, Poland.*

Digital Object Identifier 10.1109/MMM.2010.935777

for instance, dc electronic and fiber telecommunication engineers. It is not surprising, therefore, that each branch of EMs has developed its own computational methods, tailored for its particular kinds of problems.

For example, circuit theory is well established in the low-frequency spectrum. In this regime, the modeled objects are much smaller than the wavelength, and quasistatic approximations can be applied with voltages and currents instead of electric and magnetic field intensities, respectively. As the frequency increases, the wave theory becomes more adequate and, in consequence, it governs in RF, microwave, and millimeter-wave engineering. Higher up in the frequency spectrum, rigorous wave theory is still valid but becomes computationally less effective due to the large dimensions when compared to the wavelength. Thus, approximate methods tend to be applied in optics based on ray tracing, scalar/vector diffraction theory, etc.

In principle, all of the mentioned methods are based on the same physical laws of EMs, collated into a common notation by James Clerk Maxwell [2]. Numerical methods for solving Maxwell's equations in three space dimensions and time, subject to any specific boundary conditions, have attracted a lot of research interest over the last few decades. This has created a new field of knowledge called *computational EMs* and has resulted in practical EM software packages. Thus, with the aim of bridging the gap between microwaves and photonics, a natural first step appears to be adapting these software tools for higher-frequency applications.

In this article, we will focus on a number of practical examples that can give an overview of current trends in full-wave EM modeling of optical problems with

## People from distinct research areas often speak about similar phenomena using different terminologies.

the aid of the finite-difference time-domain (FDTD) method [3]. The authors of this article have several decades of experience in FDTD development. The article should be considered a review of their experience in that field rather than a comprehensive treatment of the matter. Another aim is to show that computational EM methods, like FDTD, that were originally known and well established in microwaves are now becoming feasible tools in higher-frequency spectra.

### Guided Two-Dimensional and Periodic FDTD Algorithms

There are many variants of the FDTD algorithm dedicated to the effective modeling of specific problems. Some of these variants take advantage of analytical properties of fields in a particular problem that allow one to reduce the dimensionality or size of the corresponding numerical scenario. This results in a reduction in computational effort with respect to the brute force of a full three-dimensional (3-D) FDTD simulation of the original problem.

A popular class of algorithms with reduced dimensionality comprises various two-dimensional (2-D) FDTD schemes, such as scalar 2-D [4], guided 2-D [5], or axisymmetrical 2-D [5]. See "Guided-2-D FDTD Method" for the definition of that method. Various applications of the axisymmetrical 2-D FDTD method have been discussed in a recent paper [6]. Here, we

### Guided-2-D FDTD Method

Consider a structure uniform in the  $z$ -direction. Its  $xy$ -cross-section may be as simple as that of a rectangular waveguide or as complicated as that of the photonic crystal (PhC) fiber in Figure 3(b)—the key point is that the cross-section remains identical at any  $z$  coordinate. The Fourier transform is applied in the  $z$ -dimension decomposing each field component  $G$  into a spectrum of forward and backward propagating waves:

$$G(x, y, z, t) = g(x, y, t) e^{\pm j(\beta z + \varphi)},$$

where  $g(x, y, t)$  is a real-valued function and  $\beta$  denotes the propagation constant. Waves corresponding to different values of  $\beta$  do not couple and hence can be analyzed separately. Moreover, for each traveling wave, the components  $E_z$ ,  $H_x$ , and  $H_y$  are all in phase, and shifted by  $90^\circ$  with respect to the components  $H_z$ ,  $E_x$ , and  $E_y$ .

Note that full information about the geometry is provided by its cross-section. Moreover, discretization along the  $z$ -axis is not needed, since multiplication by

$\beta$  analytically produces all  $z$ -derivatives of transverse field components required by Maxwell's equations, also compensating the  $90^\circ$  phase shift between  $H_x$ ,  $H_y$ , and  $E_x$ ,  $E_y$ . We can therefore suppress the exponential term in the above Fourier expansion and fully solve the problem in two spatial dimensions in time in terms of real functions  $g$  for any assumed value of parameter  $\beta$ . The problem is spatially 2-D, but different from the classical (scalar) 2-D problems in that all six field components may mutually couple and need to be included in the simulation. It has been proposed in [5] to denote such problems as vector 2-D ones. A vector 2-D problem reduces to a scalar 2-D problem when  $\beta = 0$ , i.e., at the mode cut-off.

In fact, the class of vector 2-D problems spans a much broader range of applications than guided waves. These are beyond the scope of the present article, but examples can be found in the original reference [5] as well as a recent review of axisymmetrical vector 2-D modeling [6].

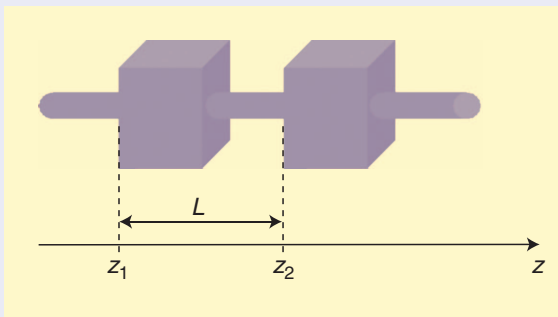
## Technological advances observed in the last century have been closely related to the dynamically growing knowledge about physical properties of electrons in solid-state materials.

shall consider scalar and guided 2-D FDTD algorithms for EM modeling of optical problems.

Another class of FDTD algorithms utilizes the Floquet theorem [7] for periodic structures. This leads to

### Periodic FDTD Method

Consider a structure periodic in the  $z$ -direction, where periodicity may be cascaded as in the figure below or continuously, as in sinusoidally corrugated waveguides. In either case, no single  $xy$ -cross-section fully represents the 3-D geometry, but a sample of a single period (or multiple periods) does.



Schematic view of a periodic structure with period  $L$ .

The Floquet theorem [7] implies that any field component  $G$  may be written as:

$$G(x, y, z, t) = g(x, y, z, t) e^{\pm j(\beta_0 z + \varphi)},$$

where  $g(x, y, z, t)$  is a real-valued function periodic with period  $L$  and  $\beta_0$  denotes a *fundamental* propagation constant of a particular wave. Note that any such wave also comprises an infinite series of spatial harmonics propagating with  $\pm\beta_0 \pm 2m\pi/L$ ,  $m = 1, 2, 3, \dots$ . Hence, the solution cannot be sought for a single value of  $\beta_0$  individually.

However, periodicity of function  $g$  allows us restrict the analysis to a single period of the structure, for example, spanning the FDTD mesh between coordinate  $z_1$  and  $z_2$ , where the tangential  $E_x, E_y$  fields (further denoted by  $E_{\perp}$  for compactness) are defined. In one FDTD implementation (denoted in the literature as the CL-FDTD method [9]), these tangential electric fields are updated in a regular manner starting at coordinate  $z_1$  and terminating at  $z_2 - \Delta z$ . Tangential

so-called periodic boundary conditions (PBC), which allow the representation of an infinite periodic structure by its FDTD model over just one period [8], [9], [10]. See "Periodic FDTD Method" for a definition of that method.

In the following sections, scalar 2-D, guided 2-D, and periodic FDTD simulations will be discussed. Examples concerning photonic crystals (PhCs), microstructured optical fibers, and scatterometry of integrated circuits (ICs) are analyzed with FDTD formulations [11]. In the final example, the 2-D FDTD algorithm is hybridized with a scalar Fresnel

magnetic fields at  $z_1 - 0.5\Delta z$  needed for electric field updates at  $z_1$  are obtained by complex backward looping from  $z_2 - 0.5\Delta z$ , as follows from the above Floquet expansion:

$$\begin{aligned} H_{\perp}(x, y, z_1 - \Delta z/2, t + \Delta t/2) \\ = H_{\perp}(x, y, z_2 - \Delta z/2, t + \Delta t/2) \exp(-j\psi), \end{aligned}$$

where  $\psi = \beta_{z0}L$  is the fundamental Floquet phase shift per period  $L$ . Similarly, tangential magnetic fields are updated in a regular FDTD manner starting at coordinate  $z_1 + 0.5\Delta z$  and terminating at  $z_2 - 0.5\Delta z$ , with the tangential electric fields needed for the last update obtained by complex forward looping:

$$E_{\perp}(x, y, z_2, t) = E_{\perp}(x, y, z_1, t) \exp(j\psi).$$

Numerical analysis is performed over one spatial period typically using complex notation for the fields, to accommodate general complex values of the looping factors.

Various periodic FDTD formulations are known from the literature. Early papers advocated *sin/cos* [42] or "split-field update" techniques [43]. The former was considered monochromatic. The latter needed new field quantities to be defined instead of the original electric and magnetic field intensities. Its advantage resided in a possibility to analyze wideband oblique illumination, however, it was likely to produce unstable solutions for grazing incidence angles. More recently, Spectral-FDTD [44] and FDTD dedicated to leaky wave analysis [45] have been proposed. They are extensions of the *sin/cos* concept, and are similar to the CL-FDTD algorithm discussed here. The method of [45] is advantageous as it allows direct extraction of complex propagation constants.

The Complex Looped FDTD has been used in this article due to its proven stability properties being the same as for the standard FDTD method. More details may be found in [9].

diffraction approach for the effective analysis of lens imaging of subwavelength objects.

## Photonic Crystal Devices

Technological advances observed in the last century have been closely related to the dynamically growing knowledge about physical properties of electrons in solid-state materials, such as crystals. Regular composition of molecules in crystals creates energy gaps for electrons. This leads to an opportunity for building diodes, transistors, and more complex electronic devices. Recently, an analogous concept has become very popular in photonics, with a view to controlling the flow of photons and building alternative devices to electronic ones.

The idea consists of producing a so-called PhC that interacts with photons in a similar way as a solid crystal interacts with electrons, though on a different spatial scale. PhCs are typically formed with two dielectrics of different refractive indices and arranged alternately into a lattice that is periodic along one, two, or three dimensions. A proper design of such PhC produces a photonic band gap (PBG), indicating energies (frequencies) of photons where the propagation inside the PhC is prohibited (in other words, EM waves are evanescent). This specific feature allows one to build devices such as planar waveguides [12], channel-drop filters [13], or couplers [14], to name a few.

The FDTD method, supplemented with PBC, is a highly relevant tool for investigating EM properties of PhC compositions. There are also other numerical methods that find application in the modeling of PhC structures, including finite-difference frequency-domain [15] or plane wave expansion [16] methods.

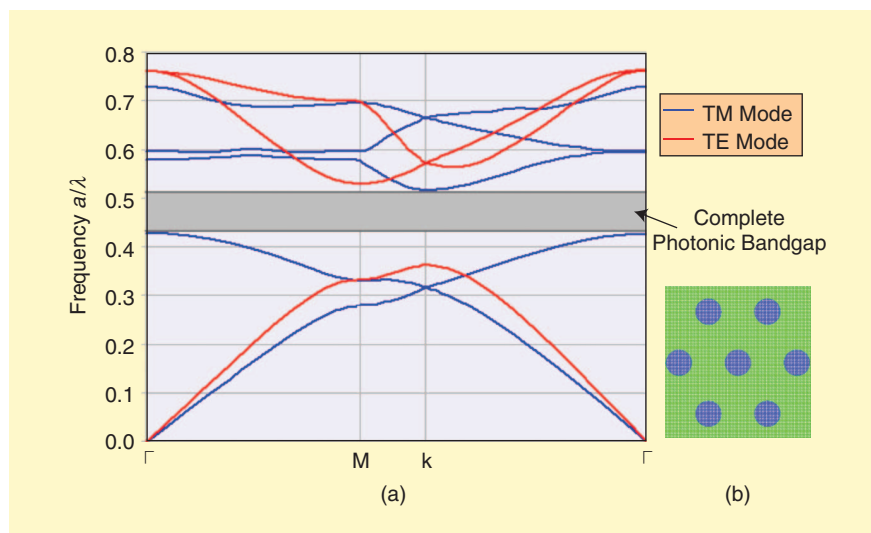
Consider a planar 2-D hexagonal air-hole lattice produced in gallium arsenide ( $\epsilon_r = 13$ ), as shown in Figure 1(b) [17]. The lattice constant and the air-hole radius are  $a = 1 \mu\text{m}$  and  $r = 0.48 \mu\text{m}$ , respectively. When the aim is to consider dispersion properties of modes with transverse electric (TE) or transverse magnetic (TM) polarization, the model can be reduced to a single layer of FDTD cells between magnetic or electric boundary conditions, respectively. This simplifies the FDTD algorithm to a scalar 2-D one. Electric and magnetic field components are then looped at the sidewalls of the model using PBC, so that only a scalar 2-D periodic FDTD model of a single periodic cell of Figure 1(b) remains to be analyzed.

## Another advantage of a time-domain approach is that the user can dynamically monitor the EM wave propagation as the simulation is running.

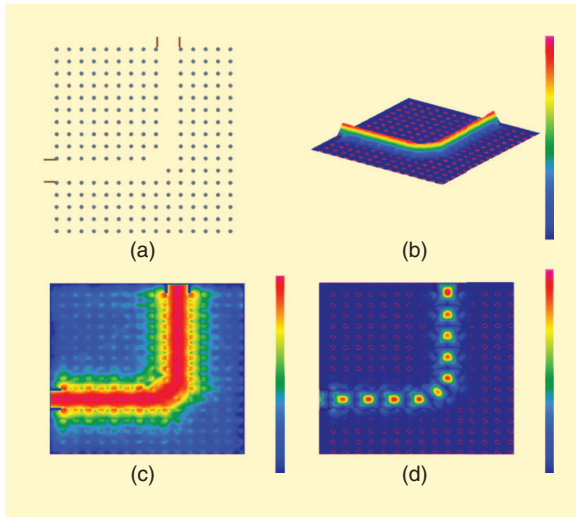
With the FDTD cell size set to 8 nm, the whole model consists of about 85,000 FDTD cells, occupying 25 MB of RAM. A single simulation with a particular set of Floquet phase shifts (defined in "Periodic FDTD Method") imposed across the periodic boundaries, a virtual pulse source, and Fourier transform coprocessing of a selected field component, yields the frequencies, where different modes can propagate in the structure, satisfying the assumed phase shifts [18]. Such a simulation takes about 20 seconds on an Intel Core2 Duo CPU 3 GHz (10 seconds on Intel Core i7 with multithreading [19]). To obtain a complete photonic band gap diagram within the first Brillouin zone [17], as shown in Figure 1(a), about 30 simulations were carried out [18].

Figure 1(a) shows that the investigated hexagonal lattice exhibits a complete photonic band gap for  $a/\lambda$  ratios between 0.428 and 0.518. This means that no TE or TM wave can penetrate the structure within this photonic band gap. The obtained solution is scalable, i.e., one can manufacture such a PhC slab for optical applications as well as for the other frequency regions, providing that materials with appropriate dielectric properties are available.

The photonic band gap phenomenon can also be exploited to guide photons in planar circuits more efficiently than using other technologies based on total internal reflection (TIR). Figure 2(a) depicts the scenario with a sharp bend in a planar PhC waveguide



**Figure 1.** (a) Photonic bandgap diagram for the hexagonal air-hole lattice shown in (b), which is manufactured in GaAs ( $\epsilon_r = 13$ ,  $a = 1 \mu\text{m}$ ,  $r = 0.48 \mu\text{m}$ ).



**Figure 2.** (a) Top view of a planar photonic crystal waveguide bend made of dielectric rods ( $\epsilon_r = 11.56$ ,  $a = 0.58 \mu\text{m}$ ,  $r = 0.104 \mu\text{m}$ ) as modeled by the authors of this article in the finite-difference time-domain software [11] based on the concept described in [20]. (b) Snapshots taken from our finite-difference time-domain simulation's envelope of the Poynting vector at  $\lambda = 1.55 \mu\text{m}$  on linear and (c) logarithmic scales. (d) Instantaneous pattern of the Poynting vector at  $\lambda = 1.55 \mu\text{m}$  on a linear scale.

hollowed in a rectangular lattice of dielectric rods ( $\epsilon_r = 11.56$ ) [20]. The lattice constant and the rod radius are  $a = 0.58 \mu\text{m}$  and  $r = 0.104 \mu\text{m}$ , respectively.

Here, the aim is to consider a TM polarized wave propagating at  $\lambda = 1.55 \mu\text{m}$ . The model is, therefore, simulated with the scalar 2-D FDTD algorithm terminated by electric boundary conditions in the third dimension. The model is supplemented with input and output ports where a desired mode is numerically injected and received, utilizing the concept of modal templates [21]. With FDTD cell size set to 25 nm, the model consists of about 275,000 FDTD cells occupying about 48 MB of RAM.

As we can see in Figure 2(b)–(d), power is concentrated in the waveguiding area. Moreover, only a small amount of reflections are generated at the bend, as demonstrated by the Poynting vector envelope that is practically flat along the direction of wave propagation.

Due to its time-domain character and taking advantage of the generalized system of  $S$ -parameter extraction after [21], the 2-D FDTD method enables investigation of such devices over a wide spectrum in a single simulation run. The dispersive dependence of applied materials can be accounted for by applying special dispersive models [22], [23].

Another advantage of a time-domain approach is that the user can dynamically monitor the EM wave propagation as the simulation is running. This provides insight into the EM phenomena, facilitating design and optimization processes.

## Microstructured Optical Fibers

Another application of PhCs can be found in the telecommunication fibers industry. Originally, propagation of light along fiber has been based on the TIR phenomenon with the refractive index of the cladding being lower than that of the core. Fibers have revolutionized modern telecommunications, successfully replacing other forms of wired data transmission in the most challenging technology areas. However, a disadvantage of those classical clad fibers lies in the difficulty to control and compensate for their dispersion characteristics. This limits the bandwidth of the propagating pulses and, by consequence, limits the maximum bit rate that can be transmitted via a single fiber core with an acceptable bit error rate (BER) level. In contrast, the application of a PhC structure as a cladding for the guiding core enables easier control of the dispersion characteristics of such PhC fibers (PCF) [24].

Direct 3-D FDTD modeling of PCFs, though possible, is still very time consuming due to their large dimensions with respect to the wavelength. Usually, the cross-section area is larger than  $20\lambda \times 20\lambda$ .

However, the guided-2-D FDTD algorithm may be easily applied [5]. This method can be used to investigate modal properties of the PCF, reducing the numerical model to the PCF cross-section and incorporating particular propagation constant analytically. However, the FDTD method is not the only possible modeling method for PCFs. Some alternatives are plane-wave expansions [25], the finite element method [26] and the finite-difference frequency-domain method [27], to name a few.

Figure 3(a) shows a cross-section of an example hexagonal air-hole PCF manufactured in silica ( $\epsilon_r = 2.1025$ ) [28]. The lattice constant and the air-hole radius are  $a = 2.3 \mu\text{m}$  and  $r = 0.5 \mu\text{m}$ , respectively. The guided-2-D FDTD method [5] enables determination of the effective refractive index of each mode propagating in the considered PCF.

We will concentrate on the fundamental mode having an electric-field distribution shown on a logarithmic scale in Figure 3(b). Due to the symmetry of the mode, the FDTD model has been reduced to one quarter of the PCF cross-section, with magnetic and electric boundaries set on the cuts. At the external sides of the fiber, Mur boundary conditions with superabsorption [29] were imposed. Figure 3(c) depicts the FDTD results compared to the independent results published in [28].

High accuracy must be ensured during FDTD simulations. Even a small error in an extracted effective modal index curve may significantly corrupt the final waveguide dispersion curve [Figure 3(d)], which is proportional to the second derivative of the effective modal index. Two measures have therefore been taken to increase the simulation accuracy. First, a fine FDTD cell size of 30 nm has been applied, generating a model

that consists of about 830,000 FDTD cells. Second, each analysis has been run until the results have fully stabilized. With the simulation speed of about 180 iterations per second (360 on Intel Core i7 with multithreading [19]), the computation of each single point of the effective refractive index dispersion curve takes only about 30 min (15 on Intel Core i7 with multithreading [19]) on the previously mentioned PC occupying about 33 MB of RAM.

Waveguide dispersion in the optical C band ( $\lambda = 1.55 \mu\text{m}$ ) amounts to about  $D = 35 \text{ ps/nm/km}$  and rapidly changes around that wavelength. Playing with the PhC geometry, one can modify that characteristic for specific purposes. One popular practice is to compensate material dispersion with waveguide dispersion. Another is to insert a section of fiber having a modified dispersion characteristic. By compensating for dispersion in the complete propagation channel, higher transmission rates are enabled.

### Scatterometry

For many decades, the semiconductor industry has been pushing forward the limits of technology by accelerating the speed of electronic devices. This is mostly due to the shrinking dimensions of the features processed on a wafer. Currently, devices processed in 45-nm technology are available on the market and new technology nodes are being developed at 32 and 22 nm. However, both current and upcoming technology nodes are well below the resolution limit of state-of-the-art classical imaging methods, where common metrology tools were applied to control the lithography process. This is one of the reasons for increasing interest in alternative nonimaging metrology techniques like scatterometry [30].

A schematic view of a typical scatterometer is shown in Figure 4. Briefly, the fundamental idea of this technique is to illuminate special metrology targets processed on a wafer with a wideband beam of light and, afterwards, measure the intensity of a mostly specular (mirror-like) reflected beam. Targets are usually composed of line gratings processed with lithography in one or more layers. Assuming that the spectrum of the reflected beam contains information about the target geometry, it is possible to extract such parameters as the line width or the overlay [31] between gratings.

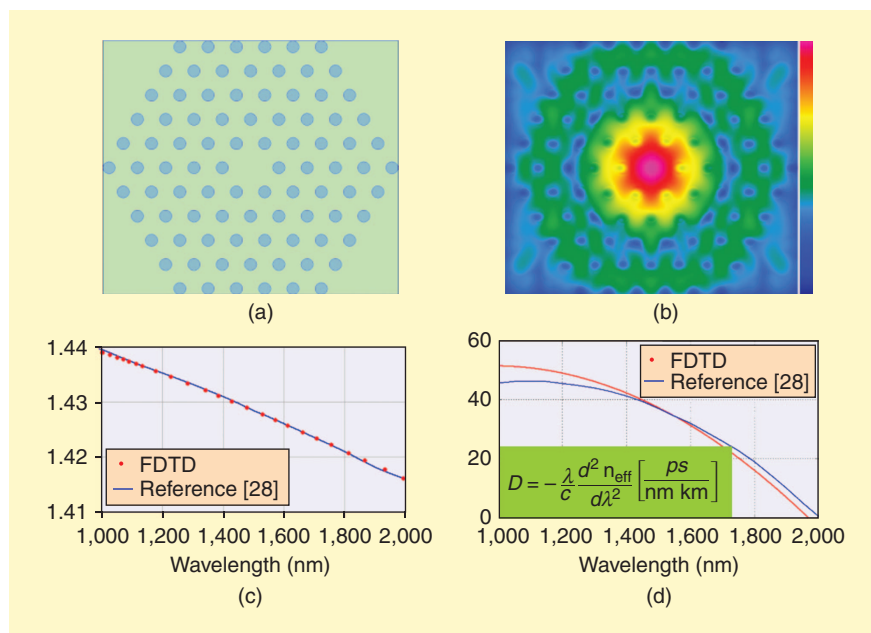


**Figure 3.** (a) Cross-section view of a hexagonal air-hole photonic crystal fiber as modeled by the authors of this article in the finite-difference time-domain software [11] based on the concept described in [28] ( $\epsilon_r = 2.1025$ ,  $a = 2.3 \mu\text{m}$ ,  $r = 0.5 \mu\text{m}$ ). (b) Results of our finite-difference time-domain simulation's envelope of the electric field at  $\lambda = 1.55 \mu\text{m}$  on a logarithmic scale, (c) effective modal refractive index, and (d) waveguide dispersion characteristic for the considered fundamental mode.

The FDTD method can be successfully applied to the modeling of such scatterometry scenarios. Assuming that the illumination beam covers many lines of the target, the problem can be approximated with an infinite periodic scenario illuminated with an unbounded plane wave. This enables reduction of the FDTD model to a single period of the target with PBC applied along the periodicity axis [32].

Figure 5(a) presents a typical target with two grating layers processed on a silicon wafer. The top grating is made of photoresist and the bottom one is processed with silica in the silicon substrate. The pitch of the gratings is set to 320 nm and line-to-space ratio is  $L/S = 1/1$ . The aim is to first illuminate the target with TE-polarized light (electric field longitudinal to the lines) at an angle of  $\phi = 25^\circ$  measured in the  $xy$ -plane from the normal to the wafer surface and then extract spectrum of the reflection coefficient.

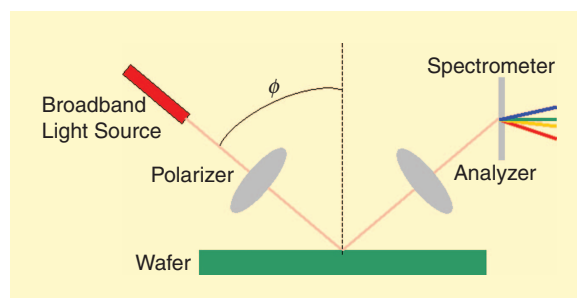


**Figure 4.** A schematic view of a scatterometry tool.

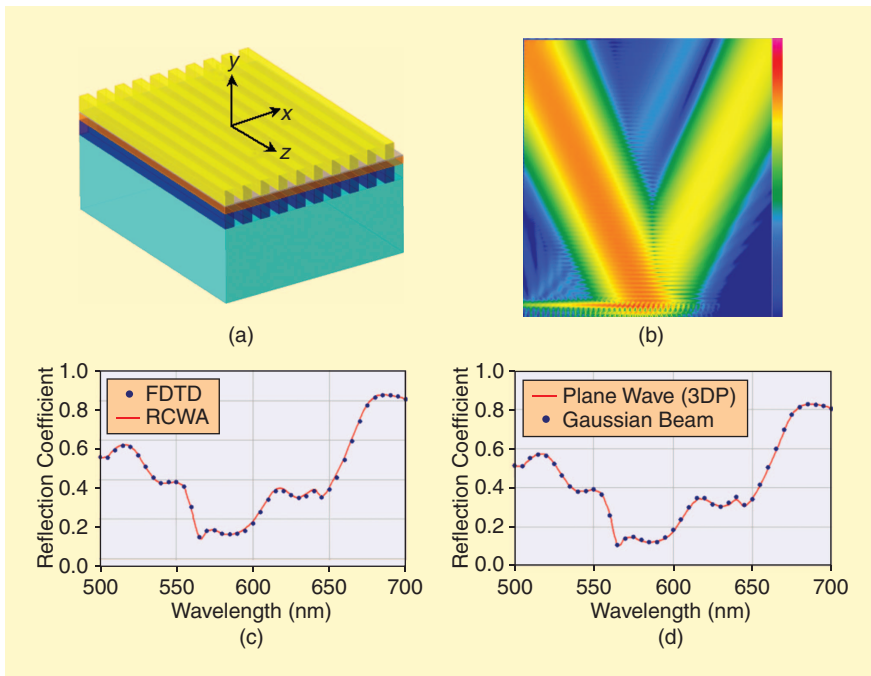


**Figure 5.** (a) A typical scatterometry target as modeled by the authors of this article in the finite-difference time-domain software [11]. (b) Results of our finite-difference time-domain simulation's envelope of the Gaussian beam (on a logarithmic scale) incident upon the target. (c) Spectrum of the reflection coefficient for infinite and (d) finite case.

Because in the considered case there is no field variation along the lines of the target, the model can be reduced to the scalar 2-D FDTD, consisting of the target cross-section placed between electric boundaries. Furthermore, application of PBC reduces the model to a single pitch. Both top and bottom sides of the model are truncated with superabsorbing Mur boundary conditions [29]. A near-to-far (NTF)-field [3] transformation is performed on a surface above the target to acquire the far-field scattering pattern and compute the reflection coefficient.

The whole FDTD model with 27,000 FDTD cells requires about 26 MB of RAM. Figure 5(c) shows the obtained results against rigorous coupled-wave analysis (RCWA) [33] and very good agreement can be observed [32], [34]. The main advantage of FDTD approach, with respect to the better-established RCWA, is that nonrectangular geometries can easily be considered. Arbitrary illumination, other than that of plane waves, can be applied as well.

Both periodic FDTD and RCWA assume that the problem is infinite, i.e., an infinitely long target is illuminated with an unbounded plane wave. In the scatterometry tools used in the IC industry, a finite periodic target is illuminated with a beam of finite spot size.

To validate the periodic approach, the 2-D FDTD algorithm is applied to a practical scenario comprising 50 pitches. All sides of the model are truncated with superabsorbing Mur boundary [29], where a NTF-field transformation is applied to compute the reflection coefficient. The whole FDTD model with

approximately 1.1 million FDTD cells requires about 176 MB of RAM. The target is illuminated with a finite spot having a Gaussian profile. The Gaussian beam diameter has been set to  $4\ \mu\text{m}$ .

Figure 5(b) depicts an example envelope of the Poynting vector distribution on a logarithmic scale. Figure 5(d) presents the calculated reflection coefficient, compared with the results obtained with the periodic FDTD simulations. Good agreement confirms validity of the periodic FDTD algorithm in this case. The Gaussian beam approach further enables the study of the impact of a diminishing spot size on the accuracy and variability of the scatterometry technique. It also enables detection of the effects of imperfect periodicity.

Recently, extensions of the periodic FDTD algorithm to the modeling of a finite source over an infinite structure have been published. The technique shown in [35] and [36] enables the investigation of EM diffraction of a spatially restricted beam in an infinite periodic geometry by considering only a single period with the PBC imposed. The method can be more efficient than the approach described above for modeling of Gaussian beam illumination of an infinite periodic structure. However, it cannot model finite dimensions of the target and possible diffraction of the beam from the edges.

### Hybrid FDTD-Fresnel Modeling of Lens Imaging Phenomenon

Optical lens imaging is a typical problem where brute force full-wave modeling is still computationally impossible because the length of entire problem space can be measured in thousands of wavelengths. Therefore, alternative numerical algorithms are used instead, based on approximate methods like ray tracing or diffraction optics [37]. However, these methods are likely to fail when geometrical details become comparable to the operating wavelength, as often happens when the target has a complicated geometry. This is the main reason for the growing popularity of hybrid computational methods that combine different algorithms to make a tradeoff between accuracy and computation time.

Literature concerning applicability of the FDTD method to modeling of far-field imaging problem is

very limited, due to the size considerations discussed above. Some published results can be found in the field of breast cancer detection [38], however, this follows a different approach to the imaging concept without utilizing focusing elements like lenses. In 2004, a paper about hybrid FDTD-Fresnel imaging of living tissues (embryo) was published [39]. Another discussion of hybrid FDTD-Fresnel modeling can be found in [40], addressing the issue of EM modeling of a confocal 3-D imaging of the subwavelength features.

One possible approach to EM modeling of lens imaging is to apply the FDTD method in the close vicinity of the target where full-wave EM modeling is necessary. The remaining part of imaging path is analyzed with a less computationally intensive method, for instance, one based on the scalar Fresnel diffraction theory [41]. It should be emphasized that the scalar Fresnel approach is applicable to a modeling of low-numerical aperture (NA) (see “Numerical Aperture” for a definition) imaging tools, usually less than  $NA = 0.6$ . For high-NA problems, a fully vectorial, and hence more cumbersome, method should be applied [37].

Figure 6(a) and (b) depicts a schematic view of the investigated confocal microscope in illumination and scanning modes, respectively. Unlike wide-field microscope tools, confocal imaging is capable of resolving a 3-D shape of the target.

The illumination beam is approximated in a 2-D FDTD model with a Gaussian beam [see Figure 6(d)], representing light radiated by the source through the input pinhole and focused by the objective lens onto the target [see the red lines in Figure 6(a)]. A Gaussian beam is launched as an excitation from above the target, as marked by the red Gaussian beam wall (GBW) line in Figure 6(c). Afterwards, a NTF-field transformation is performed on a surface above the target [green line in Figure 6(c)] to acquire the far-field scattering pattern. This is further coupled to another algorithm based on the scalar Fresnel approximation. Eventually, the light intensity distribution at the image plane is obtained.

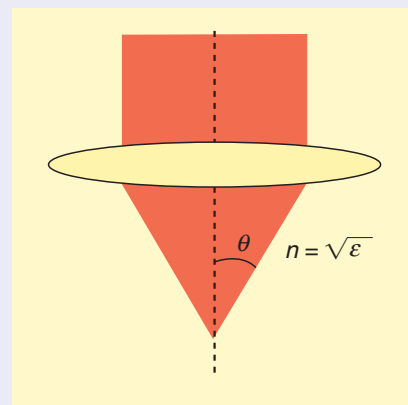
According to the concept of image formation in a confocal microscope, the above procedure has to be performed several times, shifting the beam focus horizontally and vertically around the target. The whole set of coupled

**For many decades, the semiconductor industry has been pushing forward the limits of technology by accelerating the speed of electronic devices.**

### Numerical Aperture

In microscopy, numerical aperture (NA) denotes the range of angles over which a tool can collect or radiate light. In the figure,  $n$  stands for the refractive index of the medium in which the NA is considered and  $\theta$  denotes the half-angle of the focused/emitted light cone. In most cases, the larger NA is, the better the resolution of the optical tool can be achieved.

$$NA = n \sin\theta$$



Numerical Aperture

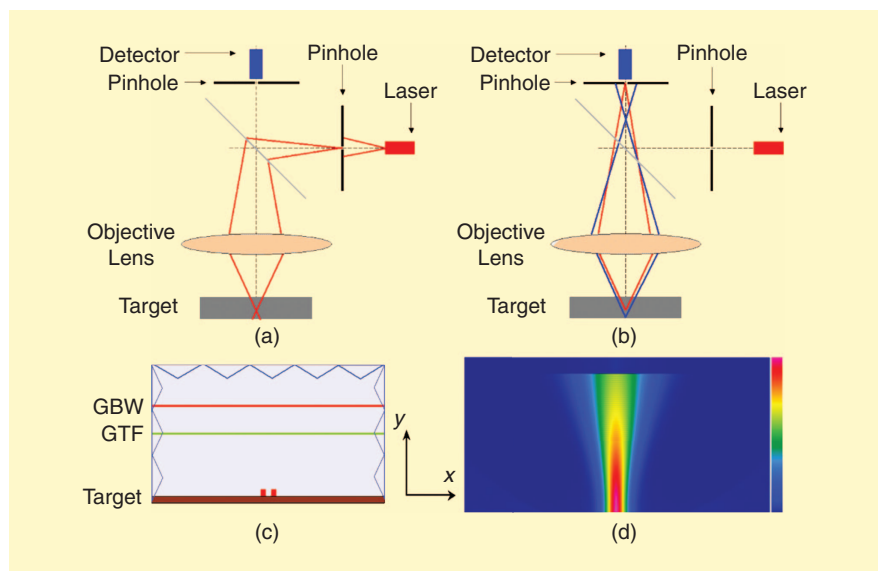


**Figure 6.** Schematic view of the confocal microscope in (a) illumination and (b) scanning modes. (c) Model prepared by the authors of this article in the finite-difference time-domain software [11] and (d) a snapshot from our finite-difference time-domain simulations showing an example envelope of a Gaussian beam (electric field).

FDTD-Fresnel simulations provide the final image pixel by pixel.

Consider the imaging of an isolated trench and line, respectively, processed in gallium arsenide ( $\epsilon_r = 10.4976$ ). The height and the width of the trench (line) are the same,  $10 \mu\text{m}$ . The length of the trench (line) extends to infinity, allowing us to apply the scalar 2-D FDTD algorithm. Assuming that the target is  $z_o = 2 \text{ mm}$  from the objective lens and the image plane is  $z_i = 200 \text{ mm}$  behind the lens, the focal length amounts to  $f_L = 1.98 \text{ mm}$ . The NA has been set to  $NA = 0.475$  ( $\theta \approx 28^\circ$ ).

The minimum FDTD cell size is set to  $10 \text{ nm}$ , ensuring at least 15 FDTD cells per operating wavelength ( $\lambda = 500 \text{ nm}$ ). The whole FDTD model is  $40 \mu\text{m}$  long [in the  $x$  direction in Figure 6(c)] to make sure that the excited Gaussian beam and the scattered field do not exceed the computational area.

A single FDTD simulation of the model, consisting of about 1.3 million FDTD cells, takes about 5 min on the previously mentioned desktop computer (2.5 on Intel Core i7 with multithreading [19]) occupying about 125 MB of RAM. The whole image has been computed with a  $1 \mu\text{m}$  step, though, due to symmetry of the targets, only half of each image has been collected. Thus, the total FDTD computation time amounts to about 24 h (12 h on Intel Core i7 with multithreading [19]).

Figure 7(a) and (b) depicts the images obtained from hybrid FDTD-Fresnel simulations developed by the authors of this article. The green lines indicate the real shape of the target. It can be noticed that the shape of each target is discernable, although, as one might expect, the axial resolution is a bit worse than the lateral one, resulting in blurred horizontal edges. Another interesting phenomenon is seen at the sharp corners of the trench (line). Due to significant dif-

fraction of the incident light at the corners of trench (line) dark vertical gaps can be observed in both images around  $x = -5 \mu\text{m}$  and  $x = 5 \mu\text{m}$ .

This example implies that the FDTD method can play an important role in the modeling of problems that are definitely beyond its computational capabilities at the moment. The presented hybrid methodology can be easily extended to the more advanced and complicated scenarios both in the FDTD and Fresnel regions.

## Conclusion

Time-domain EM software has reached its maturity for the analysis of practical microwave and millimeter wave problems. This leads to significant interest in expanding the scope of applications of the available software packages into higher-frequency ranges. Such an interest has been declared by many software developers who naturally seek new markets for their expertise and tools. But, even more importantly, interest is also being shown by engineers and entrepreneurs affiliated with the rapidly growing fields of infrared and optical technologies.

The increasing complexity of photonic and optical devices means that the classical approximate methods, for example, ray tracing or diffraction theories, often fail to provide accurate designs. On the other hand, brute force full-wave modeling, while theoretically adequate, is impractical due to typical problem sizes that are measured in hundreds or thousands of wavelengths and, hence, require prohibitive computer resources.

In this article, we have demonstrated that many representative problems of optical technologies can be accurately and effectively solved with the commercially available FDTD software, provided that such software offers the flexibility applying partial analytical knowledge to the problems. This is the case with scalar 2-D or guided 2-D FDTD algorithms relevant to the analysis of PhCs

or microstructured optical fibers, as well as periodic FDTD method applicable in the scatterometry of ICs.

We have also demonstrated an effective approach of hybridizing the FDTD and scalar Fresnel approaches for accurate and effective modeling of lens imaging phenomena. We believe that further developments along these lines using FDTD methods, supported by the concurrent developments in computer technology, will lead to hybrid time-domain software tools becoming a breakthrough in optics and photonics.

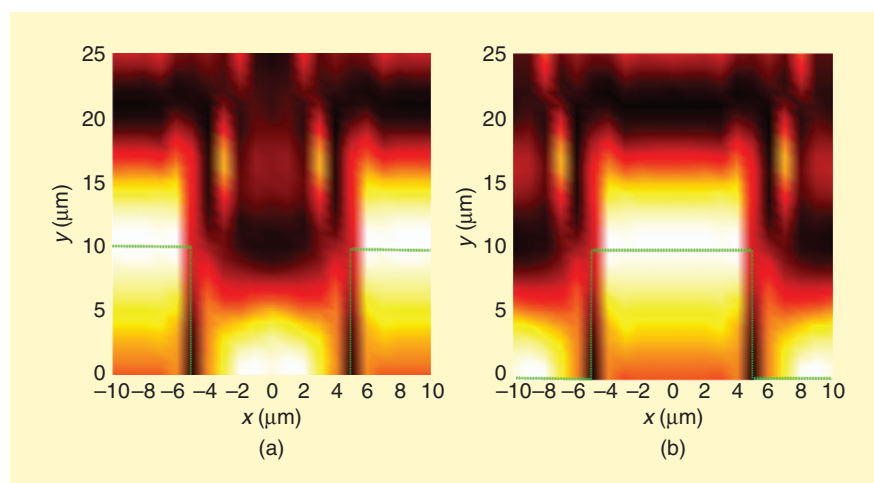


**Figure 7.** Images produced by hybrid finite-difference time-domain-Fresnel simulations of a single  $10 \times 10 \mu\text{m}^2$  target prepared by the authors of this article (a) trench and (b) line, processed in GaAs ( $\epsilon_r = 10.4976$ ) and imaged at  $\lambda = 500 \text{ nm}$  ( $f_L = 1.98 \text{ mm}$ ,  $NA = 0.475$ ).

## References

- [1] S. Weinberg, *Dreams of a Final Theory: The Scientists's Search for the Ultimate Laws of Nature*. New York: Pantheon Books, 1992.
- [2] J. C. Maxwell, "A dynamical theory of the electromagnetic field," *Philos. Trans. R. Soc. London*, 1864, vol. 155, pp. 459–512.
- [3] A. Taflove and S. C. Hagness, *Computational Electrodynamics: The Finite-Difference Time-Domain Method*. Norwood, MA: Artech House, 2005.
- [4] W. K. Gwarek, "Analysis of an arbitrarily-shaped planar circuit—A time-domain approach," *IEEE Trans. Microwave Theory Tech.*, vol. MTT-33, no. 10, pp. 1067–1072, Oct. 1985.
- [5] W. K. Gwarek, T. Morawski, and C. Mroczkowski, "Application of the FDTD method to the analysis of the circuits described by the two-dimensional vector wave equation," *IEEE Trans. Microwave Theory Tech.*, vol. 41, no. 2, pp. 311–316, Feb. 1993.
- [6] M. Celuch and W. K. Gwarek, "Industrial design of axisymmetrical devices using a customized FDTD solver from RF to optical frequency bands," *IEEE Microwave Mag.*, vol. 9, no. 6, pp. 150–159, Dec. 2008.
- [7] R. Collin, *Field Theory Of Guided Waves*. New York: McGraw-Hill, 1960.
- [8] M. Celuch-Marcysiak and W. K. Gwarek, "Effective time domain analysis of periodic structures," in *Proc. 23rd European Microwave Conf.*, Madrid, 1993, pp. 293–295.
- [9] M. Celuch-Marcysiak and W. K. Gwarek, "Spatially looped algorithms for time-domain analysis of periodic structures," *IEEE Trans. Microwave Theory Tech.*, vol. MTT-43, no. 4, pp. 860–865, Apr. 1995.
- [10] J. Maloney and M. Kesler, "Periodic structures," in *Computational Electrodynamics: The Finite Difference Time-Domain Method*, 3rd ed., A. Taflove and S. Hagness, Eds. Norwood, MA: Artech House, 2005, pp. 553–605.
- [11] (1997–2010). QuickWave-3D, QWED Sp. z o.o. [Online]. Available: <http://www.qwed.com.pl>
- [12] T. Cao, M. J. Cryan, Y.-L. D. Ho, I. J. Craddock, and C. J. Raitlon, "Fast-light based pulse compression in 2-D photonic crystal waveguides," *IEEE/OSA J. Lightwave Technol.*, vol. 25, no. 9, pp. 2590–2598, Sept. 2007.
- [13] S. Fan, P. R. Villeneuve, J. D. Joannopoulos, M. J. Khan, C. Manolatu, and H. A. Haus, "Theoretical analysis of channel drop tunneling processes," *Phys. Rev. B*, vol. 59, no. 24, pp. 15882–15892, June 1999.
- [14] Y. Shi, D. Dai, and S. He, "Proposal for an ultracompact polarization-beam splitter based on a photonic-crystal-assisted multimode interference coupler," *IEEE Photon. Technol. Lett.*, vol. 19, no. 11, pp. 825–827, June 2007.
- [15] C.-P. Yu and H.-C. Yang, "Compact finite-difference frequency-domain method for the analysis of two-dimensional photonic crystals," *Optics Express*, vol. 12, no. 7, pp. 1397–1408, Apr. 2004.
- [16] S. Xiao, L. Shen, and S. He, "A plane-wave expansion method based on the effective medium theory for calculating the band structure of a two-dimensional photonic crystal," *Phys. Lett. A*, vol. 312, no. 1–2, pp. 132–138, June 2003.
- [17] J. Joannopoulos, S. Johnson, J. Winn, and R. Meade, *Photonic Crystals. Molding the Flow of Light*, 2nd ed. Princeton, NJ: Princeton Univ. Press, 2008.
- [18] B. Salski, M. Celuch, and W. Gwarek, "Review of complex looped FDTD and its new applications," in *Proc. 24th Annu. Review of Progress in Applied Computational Electromagnetics*, Apr. 2008, pp. 557–561.
- [19] T. Ciamulski and M. Sypniewski, "Linear and superlinear speed-up in parallel FDTD processing," in *Proc. 2007 IEEE AP-S Int. Symp.*, Honolulu, June 2007, pp. 4897–4900.
- [20] A. Mekis, J. Chen, I. Kurland, S. Fan, P. Villeneuve, and J. Joannopoulos, "High transmission through sharp bends in photonic crystal waveguides," *Phys. Rev. Lett.*, vol. 77, no. 18, pp. 3787–3790, Oct. 1996.
- [21] W. K. Gwarek and M. Celuch-Marcysiak, "Wide-band S-parameter extraction from FD-TD simulations for propagating and evanescent modes in inhomogeneous guides," *IEEE Trans. Microwave Theory Tech.*, vol. 51, no. 8, pp. 1920–1928, Aug. 2003.
- [22] A. Moryc, "Finite difference time domain electromagnetic modeling applied to dispersive and anisotropic media," *Ph.D. thesis, Inst. Radioelectron.*, Warsaw Univ. Technol., Poland, 2006.
- [23] Y. Liu, C. D. Sarris, and G. V. Eleftheriades, "Triangular mesh based FDTD analysis of two-dimensional plasmonic structures supporting backward waves at optical frequencies," *IEEE/OSA J. Lightwave Technol.*, vol. 25, no. 3, pp. 938–945, Mar. 2007.
- [24] J. C. Knight, T. A. Birks, P. St. J. Russell, and D. M. Atkin, "All-silica single mode optical fiber with photonic crystal cladding," *Opt. Lett.*, vol. 21, no. 19, pp. 1547–1549, 1996.
- [25] S. E. Barkou, J. Broeng, and A. Bjarklev, "Silica-air photonic crystal fiber design that permits waveguiding by a true photonic band-gap effect," *Opt. Lett.*, vol. 24, no. 1, pp. 46–48, 1999.
- [26] J. Wang, C. Jiang, W. Hu, and M. Gao, "Properties of index-guided PCF with air-core," *Opt. Laser Technol.*, vol. 39, no. 2, pp. 317–321, 2007.
- [27] Z. Zhu and T. G. Brown, "Full-vectorial finite-difference analysis of microstructured optical fibers," *Optics Express*, vol. 10, no. 17, pp. 853–864, 2002.
- [28] L.-P. Shen, W.-P. Huang, and S.-S. Jian, "Design of photonic crystal fibers for dispersion-related applications," *IEEE/OSA J. Lightwave Technol.*, vol. 21, no. 7, pp. 1644–1651, July 2003.
- [29] K. K. Mei and J. Fana, "Superabsorption—A method to improve absorbing boundary conditions," *IEEE Trans. Antennas Propagat.*, vol. AP-40, pp. 1001–1010, Sept. 1992.
- [30] J. McNeil, S. Naqvi, S. Gaspar, K. Hickman, K. Bishop, L. Milner, R. Krukar, and G. Petersen, "Scatterometry applied to microelectronics processing," *Microlith. World*, vol. 1, no. 6, pp. 16–22, Nov./Dec. 1992.
- [31] D. Kandel, M. Adel, B. Dinu, B. Golovanevsky, P. Izikson, V. Levinski, I. Vakshtein, P. Leray, M. Vasconi, and B. Salski, "Differential signal scatterometry overlay metrology: An accuracy investigation," in *Proc. SPIE Optical Metrology—18th Int. Congr. Photonics in Europe*, Munich, vol. 6616, June 2007.
- [32] B. Salski, M. Celuch, and W. K. Gwarek, "Evaluation of FDTD regimes for scattering from periodic structures," in *Proc. 23rd Annu. Review of Progress in Applied Computational Electromagnetics*, Verona, Mar. 2007, pp. 1815–1822.
- [33] W. Lee and F. L. Degertekin, "Rigorous coupled-wave analysis for multilayered grating structures," *Proc. SPIE, Integrated Optics: Devices, Materials, and Technologies VII*, vol. 4987, pp. 264–273, 2003.
- [34] Private correspondence with KLA-Tencor, Israel.
- [35] R. Qiang, J. Chen, F. Capolino, D. Jackson, and R. Wilton, "ASM-FDTD: A technique for calculating the field of a finite source in the presence of an infinite periodic artificial material," *IEEE Microwave Wireless Compon. Lett.*, vol. 17, no. 4, pp. 271–273, Apr. 2007.
- [36] D. Li and C. D. Sarris, "Efficient finite-difference time-domain modeling of driven periodic structures and related microwave circuit applications," *IEEE Trans. Microwave Theory Tech.*, vol. 56, no. 8, pp. 1928–1937, Aug. 2008.
- [37] M. Born and E. Wolf, *Principles of Optics*. Cambridge, U.K.: Cambridge Univ. Press, 1999.
- [38] M. M. Ney, A. M. Smith, and S. S. Stuchly, "A solution of electromagnetic imaging using pseudoinverse transformation," *IEEE Trans. Med. Imaging*, vol. MI-3, no. 4, pp. 155–162, Dec. 1984.
- [39] J. L. Hollmann, A. K. Dunn, and C. A. DiMarzio, "Computational microscopy in embryo imaging," *Opt. Lett.*, vol. 29, no. 19, pp. 2267–2269, Oct. 2004.
- [40] K. Choi, J. W. M. Chon, M. Gu, and B. Lee, "Characterization of a subwavelength-scale 3D void structure using the FDTD-based confocal laser scanning microscopic image mapping technique," *Optics Express*, vol. 15, no. 17, pp. 10767–10781, Aug. 2007.
- [41] J. Goodman, *Introduction to Fourier Optics*. Greenwood Village, CO: Roberts & Company Publishers, 2004.
- [42] W. L. Ko and R. Mittra, "Implementation of Floquet boundary condition in FDTD for FSS analysis," in *IEEE APS Int. Symp. Dig.*, July 1993, vol. 1, pp. 14–17.
- [43] M. E. Veysoglu, R. T. Shin, and J. A. Kong, "A finite-difference time-domain analysis of wave scattering from periodic surfaces: oblique incidence case," *J. Electromagn. Waves Appl.*, vol. 7, no. 12, pp. 1595–1607, 1993.
- [44] A. Aminian and Y. Rahmat-Samii, "Spectral FDTD: A novel technique for the analysis of oblique incident plane wave on periodic structures," *IEEE Trans. Antennas Propagat.*, vol. 54, no. 6, pp. 1818–1825, June 2006.
- [45] T. Kokkinos, C. D. Sarris, and G. V. Eleftheriades, "Periodic FDTD analysis of leaky-wave structures and applications to the analysis of negative-refractive-index leaky-wave antennas," *IEEE Trans. Microwave Theory Tech.*, vol. 54, no. 4, pp. 1619–1630, Apr. 2006.